Nonextensivity and universality in the earthquake preparation process

C. Papadimitriou, M. Kalimeri, and K. Eftaxias*

Department of Physics, Section of Solid State Physics, University of Athens, Panepistimiopolis, GR 15784 Zografos, Athens, Greece

(Received 18 July 2007; revised manuscript received 12 November 2007; published 3 March 2008)

We suggest that the activation of a single fault by means of preseismic electromagnetic emissions (PEME) is well-described by recently introduced models for earthquake (EQ) dynamics, which have been rooted in a nonextensive framework starting from first principles. The analysis implies that the activation of a single fault is (i) a reduced self-affine image of the regional seismicity covering many geological faults, and (ii) a magnified image of the laboratory seismicity by means of acoustic and electromagnetic emissions. Finally, we study whether characteristic signatures emerged in PEME indicating the transition to the last phase of the EQ preparation process. We use the q-Tsallis entropy as a measure of organization. Tsallis entropy gives evidence of state changes leading to the point of global instability: it detects the pattern of alterations in the preseismic electromagnetic signals and is able to discriminate between "injury levels" of the focal area. Importantly, a significant organization increase can be confirmed at the tail of the recorded PEME by means of Tsallis entropy, which is also accompanied by the appearance of persistency. We argue that these footprints may indicate the fracture of the backbone of strong entities that hinders the relative motion of the fault planes.

DOI: 10.1103/PhysRevE.77.036101 PACS number(s): 62.20.M−, 05.45.Tp, 89.75.Da

I. INTRODUCTION

A model for earthquake (EQ) dynamics consisting of two rough profiles interacting via fragments filling the gap has been recently introduced by Solotongo-Costa and Posadas (SCP) [1]. The fragments size distribution function comes from a nonextensive Tsallis formulation, starting from first principles, i.e., a nonextensive formulation of the maximum entropy principle. This nonextensive approach leads to a Gutenberg-Richter (GR) type law for the magnitude distribution of EQs. More recently, Silva *et al.* [2] have revised the model introduced by SCP [1]. Their analysis resulted in a different nonextensive GR type law. The proposed GR type laws in Refs. [1,2] provide an excellent fit to seismicities generated in various large geographic areas usually identified as "seismic regions," each of them covering many geological faults. We emphasize that the GR law is an empirical statistical law which does not say anything about a specific activated fault (EQ).

What is lacking is the description of what happened locally, i.e., as a consequence of a single event, from both the temporal and the spatial point of view [3]. Herein, we focus on the activation of a single fault by means of preseismic electromagnetic (PEM) emissions [4–8].

EQs are large-scale fracture phenomena in the Earth's heterogeneous crust. Despite the large amount of experimental data and the considerable effort that has been undertaken by the material scientists, many questions about fracture processes remain standing. Especially, many aspects of EQ generation still escape our full understanding.

Fracture induced physical fields allow a real-time monitoring of damage evolution in materials during mechanical loading. Crack propagation is the basic mechanism of material failure. The motion of a crack has been shown to be governed by a dynamical instability causing oscillations in its velocity and structure on the fracture surface. Experimental evidence indicates that the instability mechanism is that of local branching: a multicrack state is formed by repetitive, frustrated microfracturing events [9]. The rupture of interatomic (ionic) bonds also leads to intense charge separation that is the origin of the electric charge between the microcrack faces [10]. On the faces of a newly created microcrack the electric charges constitute an electric dipole or a more complicated system. Due to the crack, strong wall vibration in the stage of the microbranching instability behaves as an efficient electromagnetic (EM) emitter. Thus when a material is strained, EM emissions in a wide frequency spectrum ranging from kHz to MHz are produced by opening cracks, which can be considered as the so-called precursors of general fracture; these precursors are detectable both at a laboratory [11] and a geological scale [12,13]. Our main observational tool is the monitoring of the fractures which occur in the focal area before the final break-up by recording their kHz-MHz electromagnetic emissions. Clear kHz-to-MHz EM anomalies have been detected over periods ranging from a few days to a few hours prior to recent destructive EQs in Greece, with the MHz radiation appearing earlier than the kHz. Recent results indicate that these PEM time-series contain information characteristic of an ensuing seismic event (e.g., see Refs. [5–8,14–17].

Herein, studying PEM emissions associated with the activation of a single EQ in terms of the above-mentioned two nonextensive models of EQs [1,2] we show that the statistics of a regional seismicity is merely a macroscopic reflection of the physical processes in a single EQ source. In addition, experimental evidence indicates that the nucleation of a single EQ (fault) is also a magnified self-affine image of the laboratory seismicity by means of acoustic and EM emissions. Finally, by monitoring the temporal evolution of the q-Tsallis nonextensive entropy on PEM time series, we show a significant increase of organization in the tail of the preseismic EM activity. The emergence of high organization is also accompanied by the appearance of persistency. The appearance of both high organization and persistency may in-

*ceftax@phys.uoa.gr

dicate that the fracture process acquires a self-regulating character and to a great degree the property of irreversibility, one of the important components of predictive capability [7].

This paper is organized as follows. In Sec. II we briefly present the foundations of recently introduced nonextensive models of EQ dynamics. In Sec. III we focus on a quantitative comparison between the theoretical models presented in Sec. II and PEM emissions. In Sec. IV we examine the evolution with time of the complexity in the PEM emissions by means of Tsallis entropy. In Sec. V we study whether the activation of a single fault is a magnified image of the laboratory seismicity. In Sec. VI we refer to the possible seismogenic origin of the candidate EM precursor associated with the Athens EQ. Finally, in Sec. VII we summarize our findings.

II. NONEXTENSIVE FRAMEWORK AND MODELS FOR EARTHQUAKE DYNAMICS

In nature, long-range spatial interactions or long-range memory effects may give rise to very interesting behaviors. Among them, one of the most intriguing arises in systems that are nonextensive (nonadditive). These systems share a very subtle property: they violate the Boltzmann-Gibbs (BG) statistics, the bridge to the equilibrium thermodynamics. Inspired by multifractals concepts, Tsallis [18] has proposed a generalization of the BG statistical mechanics. He introduced an entropic expression characterized by an index q which leads to nonextensive statistics,

$$S_q = k\frac{1}{q-1}\left(1-\sum_{i=1}^{W} p_i^q\right), \tag{1}$$

where p_i are the probabilities associated with the microscopic configurations, W is their total number, q is a real number, and k is Boltzmann's constant. The value of q is a measure of the nonextensivity of the system: $q=1$ corresponds to the standard, extensive, BG statistics. Indeed, using $p_i^{(q-1)}=e^{(q-1)\ln(p_i)}\sim 1+(q-1)\ln(p_i)$ in the limit $q\to 1$, we recover the usual BG entropy

$$S_1 = -k\sum_{i=1}^{W} p_i \ln(p_i). \tag{2}$$

The nonextensive formulation (1) seems to present a consistent theoretical tool to investigate complex systems in their nonequilibrium stationary states, systems with multifractal and self-similar structures, systems dominated by long-range interactions, and anomalous phenomena among others.

The process of shock fragmentation, especially when energies are high enough, leads to the existence of long-range correlations between all parts of the object being fragmented. Then the use of a nonextensive approach seems to be adequate.

Now, we focus on the model proposed by SGP [1]. Its theoretical ingredients read as follows. (i) The mechanism of relative displacement of fault plates is the main cause of EQs. (ii) The space between fault planes is filled with the residues of the breakage of the tectonic plates, from where the faults have originated. The motion of the fault planes can be hindered not only by the overlapping of two irregularities of the profiles, but also by the eventual relative position of several fragments. Thus the mechanism of triggering EQs is established through the combination of the irregularities of the fault planes on one hand and the fragments between them on the other hand. (iv) The fragments-distribution function, and consequently the energy-distribution function, emerges naturally from a nonextensive framework starting from first principles, i.e., the maximum entropy formalism.

In the frame of the SCP model [1] the Tsallis entropy has the form

$$S_q = k\frac{1-\int p^q(\sigma)d\sigma}{q-1}, \tag{3}$$

where $p(\sigma)$ stands for the probability of finding a fragment of relative surface σ (which is defined as a characteristic surface of the system) [1]. The maximum entropy formulation for Tsallis entropy involves the introduction of the following two constraints. The first one is the normalization of $p(\sigma)$:

$$\int_0^\infty p(\sigma)d\sigma = 1 \tag{4}$$

and the other is the *ad hoc* condition about the q-mean value, which can be expressed as

$$\int_0^\infty \sigma p^q(\sigma)d\sigma = \langle\langle\sigma\rangle\rangle_q. \tag{5}$$

Finally, based on the extremization of the entropy functional, SCP obtained the following analytic expression for the energy distribution of EQs [1]:

$$\log[N(m>)] = \log N + \left(\frac{2-q}{1-q}\right) \times \log[1+\alpha(q-1)(2-q)^{(1-q)/(q-2)}\times 10^{2m}], \tag{6}$$

where N is the total number of EQs, $N(m>)$ the number of EQs with magnitude larger than m, and $m\approx\log(\varepsilon)$. This is not a trivial result, and incorporates the characteristics of nonextensivity into the distribution of EQs by magnitude. α is the constant of proportionality between the EQ energy, ε, and the size of fragment, r. More precisely, SPD assumed that $\varepsilon\propto r$.

SCP [1] successfully used the formula (6) to describe the relative cumulative number of EQs to different seismic regions:

(i) California ($q=1.65$ and $\alpha=5.73\times10^{-6}$),
(ii) Iberian Peninsula ($q=1.64$ and $\alpha=3.37\times10^{-6}$), and
(iii) Andalusian region ($q=1.60$ and $\alpha=3\times10^{-5}$).

It is very important to observe the similarity in the value of the nonextensivity parameter q for the three catalogs used. We note that the expression (6) describes the energy distribution in all detectable ranges of magnitudes very well. On the contrary, for the smallest and largest magnitudes the em-

pirical formula of GR fails to describe the seismic data [19].

As it is mentioned, Silva *et al.* [2] have revised the fragment-asperity interaction model introduced in Ref. [1]. They consider the current definition of the mean value, i.e., the so-called q-expectation value (see Ref. [20] for details). Moreover, they introduce a different scale between the size of the released relative energy ε and the size of fragment r, i.e., $\varepsilon \propto r^2$. The magnitude-distribution function deduced in their approach is given by

$$\log[N(m>)] = \log N + \left(\frac{(2-q)}{1-q}\right)\log\left[1-\left(\frac{1-q}{2-q}\right)\left(\frac{10^{2m}}{\alpha^{2/3}}\right)\right], \tag{7}$$

which is different from the one [Eq. (6)] obtained by SCP [1].

Silva *et al.* [2] successfully tested the viability of this distribution function with data in four different areas:

(i) Samambaia fault, Brazil ($q=1.60$ and $\alpha=1.3\times10^{10}$),

(ii) New Madrid fault ($q=1.63$ and $\alpha=1.2\times10^{10}$),

(iii) Anatolian fault ($q=1.71$ and $\alpha=2.8\times10^{10}$), and

(iv) San Andreas fault ($q=1.6$ to 1.7 and $\alpha\sim10^{10}$) [21].

We observe that the analyses presented in Refs. [1,2] provide almost similar q values for the two introduced nonextensive GR type laws (6) and (7). On the contrary, the parameter α differs by several orders of magnitude.

III. NONEXTENSIVITY IN THE ACTIVATION OF A SINGLE UNIT

Now, we focus on the activation of a single fault by means of precursory EM emissions. In the frame of the SCP model [1], a sequence of precursory EM pulses occurs when there is a fracture of the fragments that fill the space between the irregular fault planes of the activated individual fault.

Clear MHz-to-kHz EM emissions have been detected over periods ranging from a few days to a few hours prior to recent destructive EQs in Greece. A multidisciplinary analysis in terms of criticality [7], complexity [14,16], laboratory experiments [6–8], fault modeling [22], fractal electrodynamics [15], scaling similarities of fracturing of solid materials [6], and mesomechanics [17] validate the association of the detected preseismic EM emissions with the fracturing process in the focal area of the impending EQ.

In the present study, we concentrate on the case of the Athens EQ. A challenge in this field of research is to distinguish characteristic stages in the evolution of the precursory EM activity associated with the Athens EQ and identify them with the equivalent last stages in the EQ preparation process. In this direction, our model of the focal area consists of (i) a backbone of strong and large entities distributed along the activated fault and (ii) a strongly heterogeneous medium that surrounds the family of strong entities that prevent the free slip. Based on this model, we recently proposed the following two stages model [5,7]. The first stage, which includes the initially emerged MHz EM activity prior to the Athens EQ, originates during cracking in the highly heterogeneous material that surrounds the backbone of large and strong entities. This emission could be described in analogy with a thermal continuous phase transition [7]. The second stage includes the kHz EM radiation that emerges in the tail of the precursory EM activity and ceases approximately 9 h before the Athens EQ. This activity indicates an underlying nonequilibrium process without any footprint of an equilibrium thermal phase transition. We have suggested that this radiation is due to the fracture of the backbone that sustains the system [5,7]. Thus for the purposes of this work, we concentrate on the precursory kHz EM activities. We note that the sequence of MHz-kHz EM emissions detected prior to the Kozani–Grevena EQ, which occurred in Greece on May 13, 1995 with magnitude ($M_w=6.5$), also follows the above-mentioned two stages model [7].

The Athens EQ ($M_s=5.9$) occurred on September 7, 1999. Clear EM anomalies at 3 and 10 kHz have been simultaneously detected from a few days up to a few hours prior to this EQ (see Fig. 1 in Ref. [6]). The seismogenic origin of this EM activity has been supported by a series of papers [5–8,14–17,22]. In Fig. 1 we present the 10 kHz EM time series from July 4 up to September 9. The included candidate precursory emission emerged on September 1, 1999 [8,14]. Figure 2 focuses on the EM precursor. Figure 1 shows that the precursor launches from a long duration quiescence period concerning the detection of EM disturbances at the kHz frequency band (see Fig. 1). We concentrate on Fig. 2. We recognize the possible precursor as follows. The EM background (noise) (Epoch 1) follows the fractional Gaussian noise model [7,8]. The noise is also characterized by a low organization (or high complexity) [8,14], as it was expected. On the contrary, the accelerating candidate EM precursor (Epochs 2 and 3) follows the fractional Brownian motion (fBm) model [7,8]. Particularly, the Epochs 2 and 3 follow the antipersistent and persistent fBm model, correspondingly. Moreover, Epoch 2 is characterized by a slightly higher organization (or lower complexity) in comparison to that of the EM background, while the launch of the bursts A and B (Epoch 3) is combined with a much higher organization (or lower complexity) even in respect to that reported in Epoch 2. In Sec. VI we examine the seismogenic origin of the precursor based on a rather austere scheme including the results of the present study.

We pay attention to the following fact. Figure 2 shows that the candidate precursory activity is completed with two distinct very strong burstlike signals A and B (Epoch 3). The larger anomaly, the second one, contains approximately 80% of the total EM energy received [22]. Importantly, the fault modeling of the Athens EQ, based on information obtained by radar interferometry [23], predicts two faults: the main fault is responsible for 80% of the total energy released, while the secondary fault segment for the remaining 20%. An independent seismic data analysis has verified the aforementioned result [22]. This experimental evidence supports the hypothesis that the two distinct EM bursts originated during the activation of two separate sources (faults), namely, during the fracture of the backbone of strong and large entities that sustain the system [5,7].

The focal area of an impending earthquake is clearly an extremely complex system dominated by nonlinear interactions. As the response record of the focal area on external excitation, preseismic electromagnetic emissions (PEME)

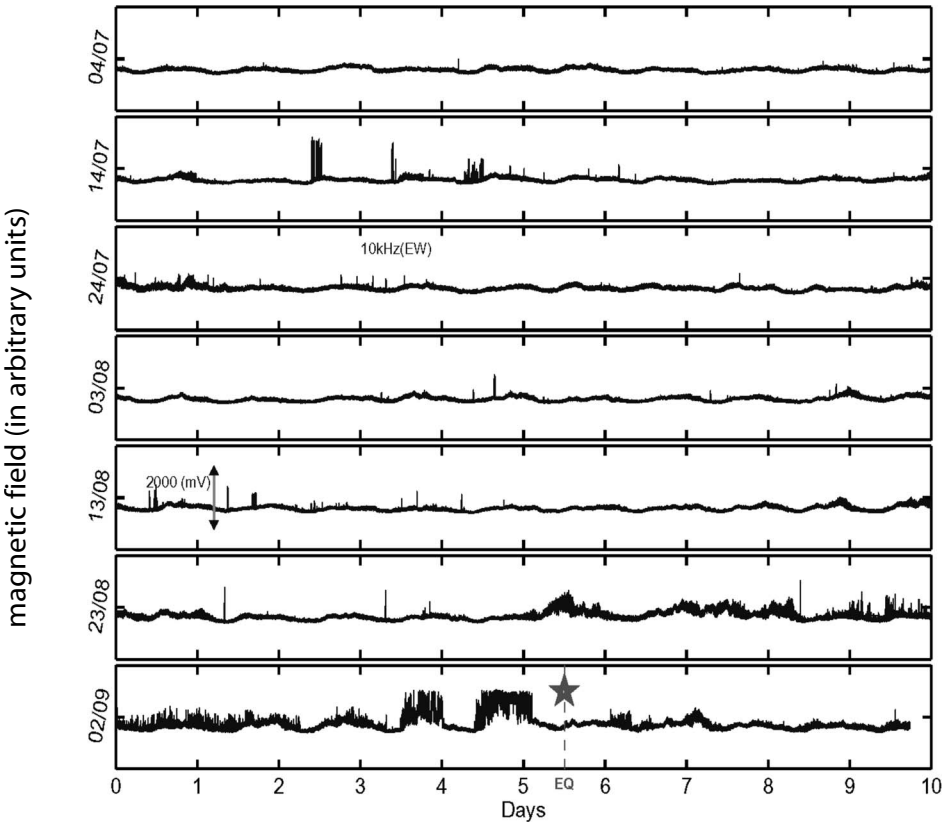

FIG. 1. Time series of the 10 kHz (East-West) magnetic field strength between July 4 and September 11, 1999 in arbitrary units. The lower star indicates the time of the Athens earthquake occurrence. A candidate precursory anomaly emerged from a few days up to a few hours before the EQ (see Fig. 2). It is clear that the candidate precursor is embedded in a long duration quiescence period concerning the detection of EM disturbances at the kHz frequency band. The Athens EQ occurred shortly after the major, M_w=7.4, Izmit, Turkey EQ that occurred on August 17, 1999. A possible relation between these two EQs may justify (i) the rather long duration of the candidate EM precursor associated with the Athens EQ, (ii) its clear launch from the noise, and (iii) the including rich prefracture information (Sec. VI).

should include much more information than the one presented previously in literature. At this point, one of the most important challenges would be to make a quantitative comparison between theoretical models and experimental results. Thus, in this contribution, such an endeavor has been made by applying the nonextensive formulation represented by Eqs. (6) and (7) to PEME, a typical kind of crackling noise [24]. More precisely, we examine whether the expressions

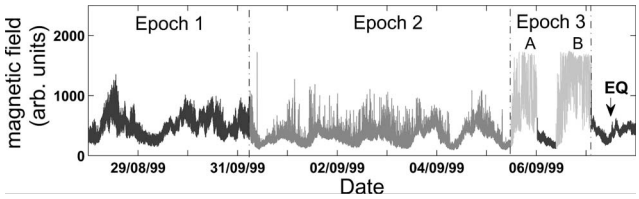

FIG. 2. View of the candidate preseismic electromagnetic emission included in the time series of the 10 kHz (East-West) magnetic field strength depicted in Fig. 1. The vertical line indicates the time of the Athens EQ occurrence. Epoch 1 refers to the EM background (noise). The noise follows the fractional Gaussian noise model and it is characterized by a low organization and high complexity [8,14]. The initial phase of the candidate precursor (Epoch 2) follows the antipersistent fractional Brownian motion model, while it is combined by a slightly higher order of organization in comparison to that of the noise [8,14]. We stress the emergence of two strong impulsive signals A and B in the tail of the accelerated precursory EM activity (Epoch 3). The bursts A and B follow the persistent fractional Brownian motion model [8,14]. Moreover, they are characterized by a significant higher organization in comparison even to that of Epoch 2 [8,14]. Numerous prefracture signatures are hidden in bursts A and B (see Sec. VII).

(6) and (7) also describe the energy distribution of the precursory "EM earthquakes" associated with the damage of fragments filling the gap between the two fault planes and hindering their relative motion.

The background (noise) level of the EM time series $A(t_i)$ is A_{noise}=500 mV [6]. We regard as amplitude A of a candidate "fracto-electromagnetic emission" the difference $A_{fem}(t_i)=A(t_i)-A_{\text{noise}}$. We consider that a sequence of k successively emerged "fracto-electromagnetic emissions" $A_{fem}(t_i)$, $i=1,\ldots,k$ represents the EM energy released, ε, during the damage of a fragment. We shall refer to this as an "electromagnetic earthquake" (EMEQ). Since the squared amplitude of the fracto-electromagnetic emissions is proportional to their energy, the magnitude M of the candidate EMEQ is given by the relation $M=\log \varepsilon \sim \log\{\Sigma[A_{fem}(t_i)]^2\}$.

Figure 3 shows that Eq. (6) provides an excellent fit to the preseismic EM experimental data, incorporating the characteristics of nonextensivity statistics into the distribution of the detected precursory EMEQs. Herein, N is the total number of the detected EMEQs, $N(M>)$ the number of EMEQs with magnitude larger than M, $G(>M)=N(M>)/N$ the relative cumulative number of EMEQs with magnitude larger than M, and α the constant of proportionality between the EM energy released and the size of fragment [1,2]. The best-fit parameters for this analysis are given by

$$q = 1.80$$

and

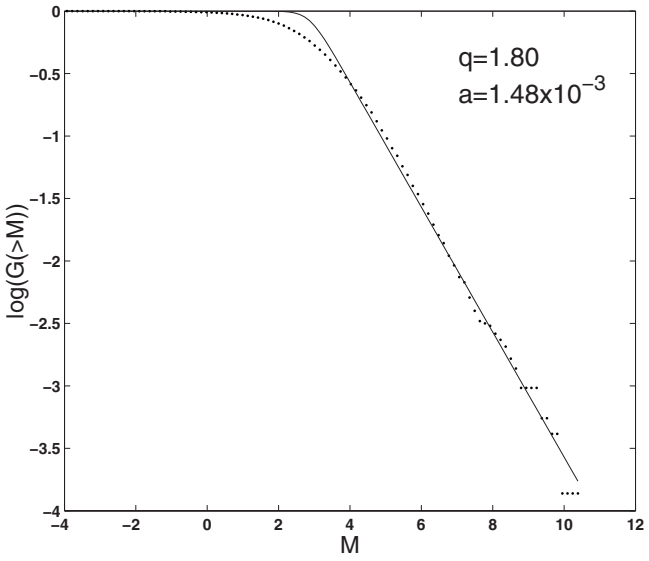

FIG. 3. We use formula (6) to calculate the relative cumulative number of electromagnetic earthquakes (see text), $G(>M)$, included in the whole precursory phenomenon, namely, in the phases P1 and P2 depicted in Fig. 2. There is an agreement of formula (6) with the data. The associated parameters are $q=1.80$ and $\alpha=1.48\times10^{-3}$.

$$\alpha = 1.48 \times 10^{-3}.$$

We focus on the second EM burst, which is associated with the activation of the main fault. Figure 4 shows that the EMEQs included in this EM burst also follow the Eq. (6). The best-fit parameters for this case are given by

$$q = 1.84$$

and

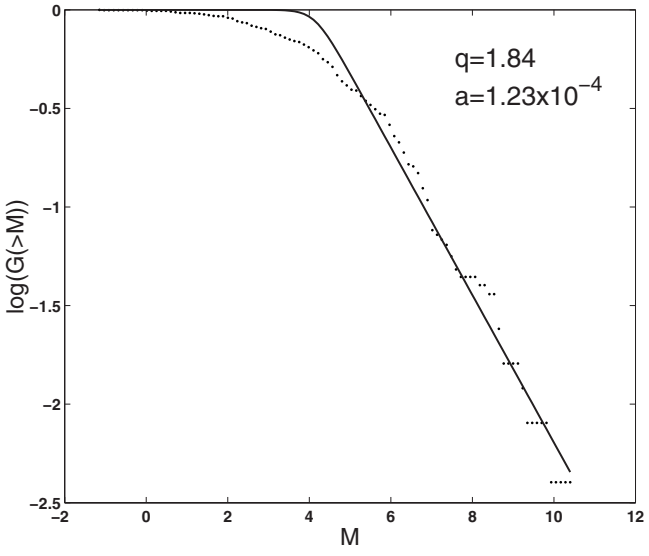

FIG. 4. We use formula (6) to calculate the relative cumulative number of electromagnetic earthquakes (see text), $G(>M)$, only included in the second strong electromagnetic burst that emerged in the tail of the precursory electromagnetic activity (see Fig. 2). There is an agreement of formula (6) with the data. The associated parameters are $q=1.84$ and $\alpha=1.23\times10^{-4}$.

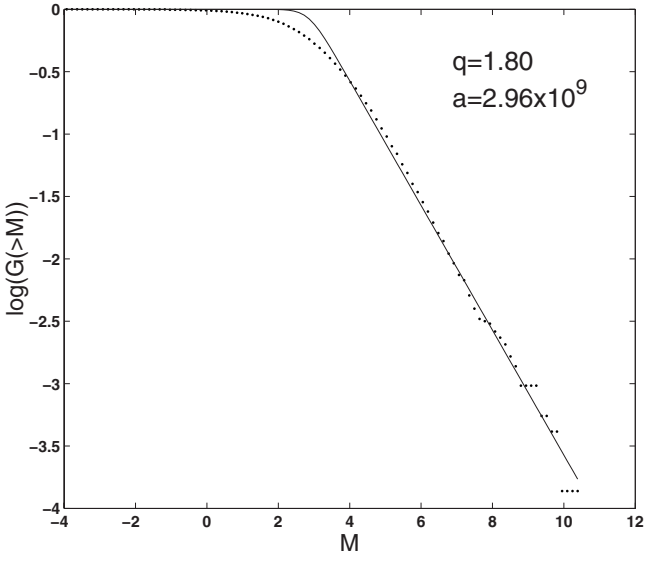

FIG. 5. We use formula (7) to calculate the relative cumulative number of electromagnetic earthquakes (see text), $G(>M)$, included in the whole precursory phenomenon, namely, in the phases P1 and P2 depicted in Fig. 2. There is an agreement of formula (7) with the data. The associated parameters are $q=1.80$ and $\alpha=2.96\times10^{9}$.

$$\alpha = 1.23 \times 10^{-4}.$$

We emphasize that Eq. (6) describes both various regional seismicities and preseismic EM activities with rather similar q-Tsallis nonextensive parameters.

Now we study the PEME in terms of the nonextensive model presented in Ref. [2]. Figure 5 shows that the formula (7) also provides an excellent fit to the preseismic EM data associated with the Athens EQ. The best-fit parameters for these analyses are given by $q=1.80$ and $\alpha=2.96\times10^{9}$. Equation (7) also fits the sequence of EMEQs included in the second EM burst (see Fig. 6) with parameters $q=1.84$ and $\alpha=3.16\times10^{13}$. We conclude that Eq. (7) also describes both different regional seismicities and sequences of EMEQs with rather similar q-Tsallis nonextensive parameters.

It is very interesting to observe the similarity in the q values associated with both nonextensive Eqs. (6) and (7) for all the catalogs of EQs used, as well as for all the precursory sequences of EMEQs under study. Though intriguing to some extent, this reveals that the obtained formulas (6) and (7) are not a mere artifact, and suggests that a more exhaustive study of the EQ nucleation in terms of nonextensive statistics is needed to give a deeper interpretation of this result. The observed similarity in the q values also indicates that the activation of a single EQ (fault) could be considered as a reduced self-affine image of the whole regional seismicity.

The entropic index q characterizes the degree of nonextensivity reflected in the following pseudo-additivity rule [18,25]:

$$S_q(A+B) = S_q(A) + S_q(B) + (1-q)S_q(A)S_q(B), \qquad (8)$$

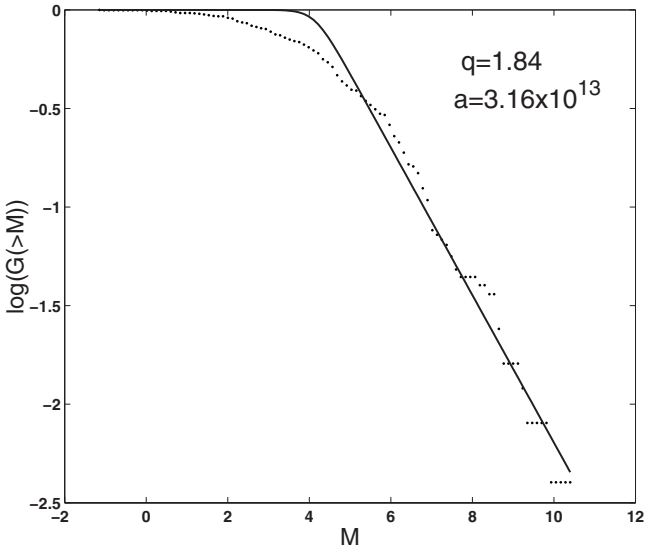

FIG. 6. We use formula (7) to calculate the relative cumulative number of electromagnetic earthquakes (see text), $G(>M)$, only included in the second strong electromagnetic burst that emerged in the tail of the precursory electromagnetic activity (see Fig. 2). There is an agreement of formula (7) with the data. The associated parameters are $q=1.84$ and $\alpha=3.16\times10^{13}$.

where A and B are two independent systems in the sense that the probabilities of $A+B$ factorize into those of A and B. The values $q>1$, $q=1$, or $q<1$ correspond to subextensivity, extensivity, or superextensivity, respectively. As it is expected, the estimated values $q>1$ represent a subextensive: the interactions and information transition across the activated fault have been verified. Notice the estimation for the nonextensive parameters is in full agreement with the upper limit $q<2$ obtained from several independent studies involving the Tsallis nonextensive framework [26].

IV. MONITORING THE EVOLUTION OF ORGANIZATION AS THE EARTHQUAKE APPROACHES

As it is mentioned, a challenge in this field of research is to distinguish characteristic epochs in the evolution of PEM activities and identify them with the equivalent last stages in the EQ preparation process. There is a recent thesis in the literature that an important organization of a physical system precedes a catastrophic event [27]. In this context, one can search for signatures that imply the transition from a normal state to a main catastrophic event (e.g., earthquake). Hereby, we attempt to demonstrate that an organization measure, such as Tsallis entropy, gives evidence of state changes leading to the point of global instability: it detects the pattern of alterations in the preseismic EM signals and is able to discriminate between the "injury levels" of the focal area.

We focus on the preseismic time series associated with the Athens EQ. The data have been recorded with a sample rate 1 sample/s. The Tsallis entropy can measure the organization of a stationary signal. Thus, starting from the raw data, we search for locally stationary and long enough time windows in the preseismic EM time series which ensure a good statistical analysis (see below). Figure 7 shows 25 separate stationary time windows each one of $N=4000$ sample points (seconds). Their stationarity has been evaluated in Ref. [14]. As the test of stationarity we have run the following algorithm. Starting from the middle of the window, we consider some subwindows around the center with an increasing radius. We consider that a window is stationary when the variation of the mean values of the subwindows is not very important (less than 5%).

The windows W1–W8, W20, W24, and W25 correspond to the EM background (noise) in the region of station, which follows the fractional Gaussian noise (fGn) model [8]. The windows W9–W16 belong to the initial part of the emerged signal that follows the antipersistent fractional Brownian motion (fBm) model [8]. Finally, the windows W17–W19 and W21–W23 are included in the final part of the precursor, i.e., into two strong EM bursts that follows the persistent fBm model [8].

We estimate the Tsallis entropy based on the concept of symbolic dynamics [28]: from the initial measurements we can generate a sequence of symbols, where the dynamics of the original (under analysis) system has been projected. This symbolic sequence can be analyzed by terms of information theory such as entropy estimations. Symbolic dynamics is based on a coarse graining of the measurements, i.e., the original EM time series of length N $(X_1,X_2,\ldots,X_N)$, is projected to a symbolic time series $(A_1,A_2,\ldots,A_N)$ with A_n from a finite alphabet of λ letters $(0,\ldots,\lambda-1)$ with

$$A_n=0 \quad \text{for } X_{\min}<X_n<x^{(0)},$$

$$A_n=1 \quad \text{for } x^{(0)}<X_n<x^{(1)},$$

$$\vdots$$

$$A_n=\lambda-1 \quad \text{for } x^{(\lambda-2)}<X_n<X_{\max}, \tag{9}$$

where x^k are positions between the minimum and maximum values $X_{\min},X_{\max}$.

After symbolization, the next step in identification of temporal patterns is the construction of symbol sequences with size L. We use the technique of lumping. Lumping is the reading of the symbolic sequence by "taking portions," as opposed to gliding, where one has essentially a "moving frame." In general, the basic novelty of the entropy analysis by lumping is that, unlike the Fourier transform or the conventional entropy by gliding, it gives results that can be related to algorithmic aspects of the sequences. Thus we stipulate that the symbolic sequence is to be read in terms of distinct successive "blocks" of length L, $A_1,A_2,\ldots,A_L/A_{L+1},\ldots,A_{2L}/A_{jL+1},\ldots,A_{(j+1)L}$.

The number of all possible blocks of length L in a λ-letter alphabet is $N_\lambda=\lambda^L$. We determine the probabilities of occurrence of each of N_λ different kinds of blocks, $p(L)_{A_1,A_2,\ldots,A_L}$ as

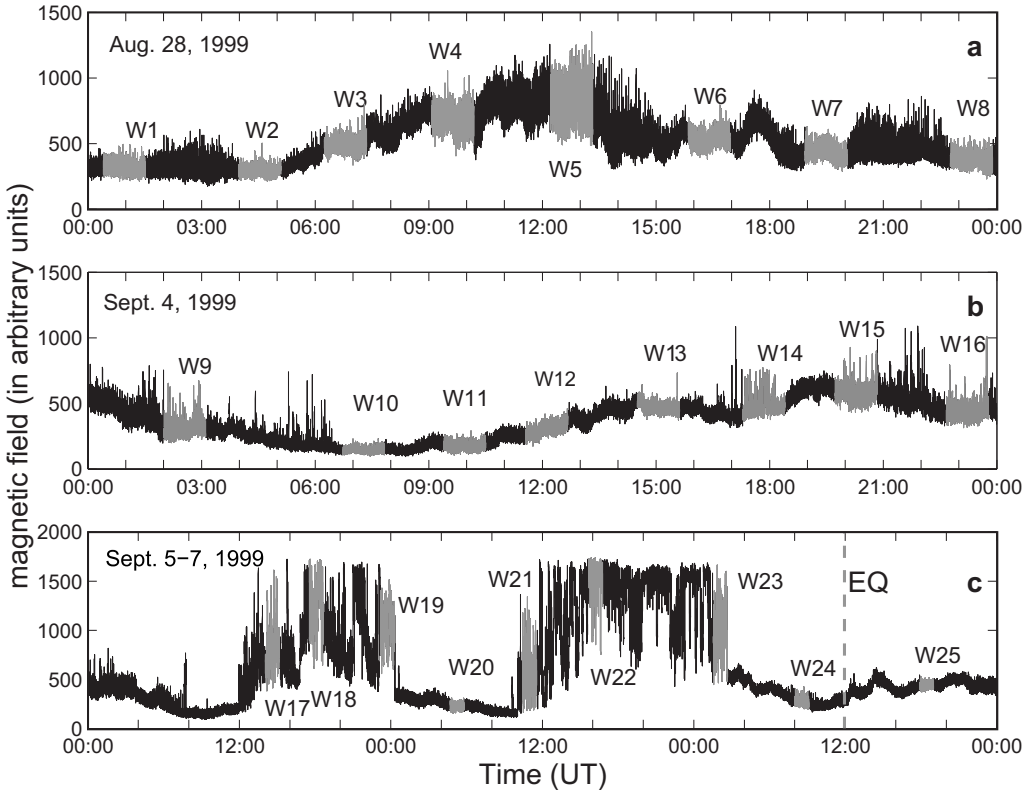

FIG. 7. View of segments of the time series of the 10 kHz (East-West) magnetic field strength shown in Fig. 1. The vertical line indicates the time of the Athens earthquake occurrence. We show the 25 time windows W1–W25, which are characterized by a good stationary behavior. Each of these windows includes 4000 samples. The data have been recorded with a sampling rate 1 sample/s.

$$p(L)_{A_1,A_2,\ldots,A_L} = \frac{\text{Number of blocks of the form } A_1,A_2,\ldots,A_L \text{ encounter by lumping}}{\text{Total number of blocks encountered by lumping}}. \quad (10)$$

To be more concrete, the simplest possible coarse graining of the preseismic signal is given by choosing a threshold C and assigning the symbols "1" and "0" to the signal, depending on whether it is above or below the threshold (binary partition). Thus we generate a symbolic time series from a two-letter ($\lambda=2$) alphabet (0, 1), e.g., 0110100110010110…. Reading the sequence by lumping of length $L=2$ one obtains 01/10/10/01/10/01/01/10/…. The number of all possible kinds of blocks is $\lambda^L=2^2=4$, namely 00, 01, 10, and 11. Thus the required probabilities for the estimation of the Tsalis entropy p_{00}, p_{01}, p_{10}, p_{11} are the fractions of the blocks 00, 01, 10, 11 in the symbolic time series.

The Tsallis entropy for the word length L is

$$S_q(L) = k\frac{1}{q-1}\left(1 - \sum_{(A_1,A_2,\ldots,A_L)} [p(L)_{A_1,A_2,\ldots,A_L}]^q\right). \quad (11)$$

Broad symbol-sequence frequency distributions produce high entropy values, indicating a low degree of organization. Conversely, when certain sequences exhibit high frequencies, low values are produced, indicating a high degree of organization.

We clarify that the real Tsallis entropy corresponds to the optimal partition. The optimal partition is the one that maximizes the Tsallis entropy. The corresponding entropy-like quantities for the other partitions are pseudo-Tsallis entropies. For this purpose, the threshold C is initially fixed to the mean value of the data in the particular time window under study. For the corresponding symbolic sequence we estimate the associated "pseudo-Tsallis entropy." We repeat the above procedure by changing the threshold c around the mean value. Our analysis indicates that the optimal partition corresponds always to a threshold not very far from the mean value of the segment.

In summary, within each of the 25 stationary time windows under study, the Tsallis entropy for $q=1.8$ is calculated by lumping for the corresponding optimal partition. We use the parameters $\{N=4000, \lambda=2, \text{ and } L=2\}$, which ensure a good statistical precision. Entropies will be systematically underestimated if the number of possible words is of the order of the ensemble size. In our analysis, this issue has minor importance after our selection of $N=4000$ because we use only short words and small alphabet. The power of these parameters to distinguish various stages of organization in

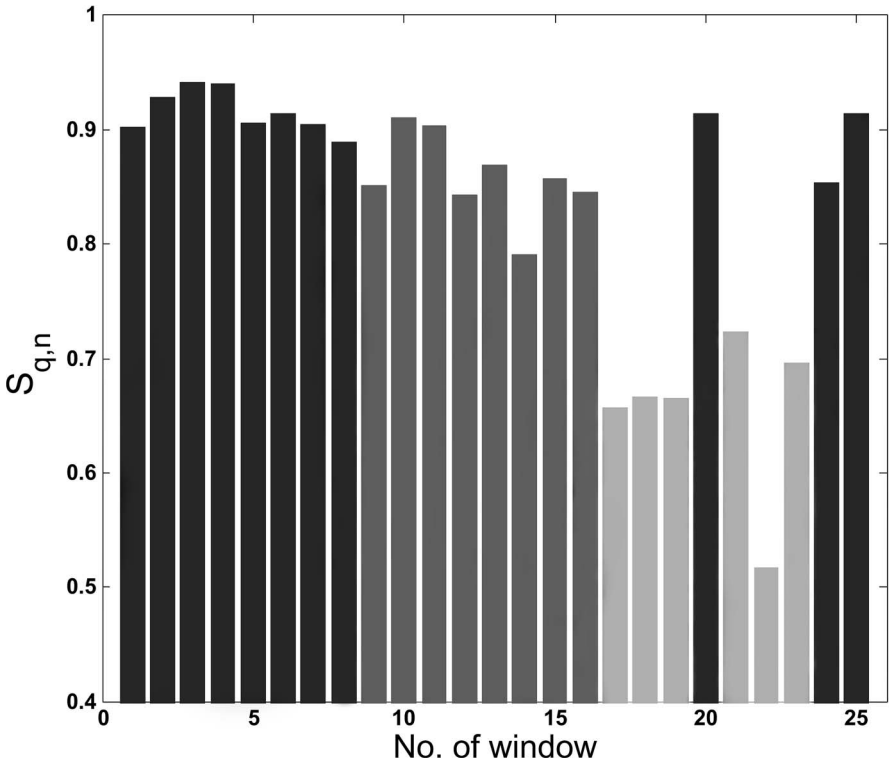

FIG. 8. The normalized q-Tsallis entropy, where $q=1.80$, for the stationary different time windows W1–W25 depicted in Fig. 7. The Tsallis entropy has been normalized with the q-Tsallis entropy for a uniform distribution of probabilities. We observe a very important reduction of the entropy inside the two strong impulsive bursts, namely within the time windows W17–W19 and W21–W23. The time series inside these two bursts also show a strong persistent behavior.

the preseismic EM activity under study has been evaluated in terms of Kolmogorov-Sinai entropy [14].

The q-Tsallis entropy with $q=1.8$ was shown to be robust enough to quantify the temporal evolution of the order-disorder of the preseismic time series. Indeed, Fig. 8 suggests the existence of three different regimes. (i) The EM background is characterized by a low organization, as it was expected [windows W1–W8, W20, W24, W25]. The EM background is also characterized by a low organization in terms of Kolmogorov-Sinai entropy [14] and approximate entropy [8], as well as by a high complexity in terms of T complexity [8] and correlation dimension [14]. (ii) We observe a slight shift of Tsallis entropies toward lower values in the initial part of the candidate EM precursor, i.e., in the windows W9–W16. This shift is also observed in terms of Kolmogorov-Sinai entropy [14] and T complexity [8]. Especially, the analysis by means of approximate entropy reveals that Epoch 2 includes a population of fracto-EM events sparsely distributed in time having a clearly higher organization in comparison to the organization of the EM background (see Fig. 11 in [8]). (iii) A sharp significant increase of organization is launched within the two strong impulsive EM emissions A and B [windows W17–W19 and W21–W23]. The analysis in terms of Kolmogorov-Sinai entropy [14], approximate entropy [8], T complexity [8], and correlation dimension [14] also reveals that the bursts A and B are characterized by a much higher degree of organization (or much lower complexity) even in respect to those reported in Epoch 2. We recall that these three different regimes were also extracted by means of the Hurst exponent [8]: the temporal evolution of the local Hurst exponent shows that the windows [W1–W8, W20, W24, W25], [W9–W16], and [W17–W19 and W21–W23] follow the fractional Gaussian noise model, the antipersistent fractional Brownian motion model, and the persistent fractional Brownian motion model, correspondingly. We underline the fact that the initial precursory epoch (Epoch 2) of lower organization (or higher complexity) corresponds to the antipersistent epoch and the final epoch (Epoch 3) of much higher organization (or lower complexity) corresponds to the persistent epoch. The power of the method of the Tsallis entropy by lumping is manifested in the fact that the method works sufficiently even after only two-symbols linguistics.

We think that, taken together: (i) the appearance of significant increase of organization by means of Tsallis entropy, (ii) the emergence of strong persistent behavior, (iii) the absence of any footprint of an equilibrium phase transition, and (iv) the excellent description of the "EM earthquakes" associated with the activation of a single fault by the nonextensive formulas [Eqs. (6) and (7)], it might be concluded that the EM precursors under study are generated by the last stage of the impending EQ, namely, during the fracture of fragments that fill the gap between the two rough profiles of the corresponding activated fault sustaining the system.

V. ACTIVATION OF A SINGLE FAULT AS A MAGNIFIED SELF-AFFINE IMAGE OF THE LABORATORY SEISMICITY

A question that effortlessly arises is whether the activation of a single EQ is not only a reduced self-affine image of the whole regional seismicity but also a magnified self-affine image of the laboratory seismicity. It would be desirable to have analyses of prefracture acoustic or EM emissions, i.e., laboratories seismicities, in terms of the nonextensive formulas [Eqs. (6) and (7)], and thus to compare the corresponding q values with the ones found in Refs. [1,2] and in this work.

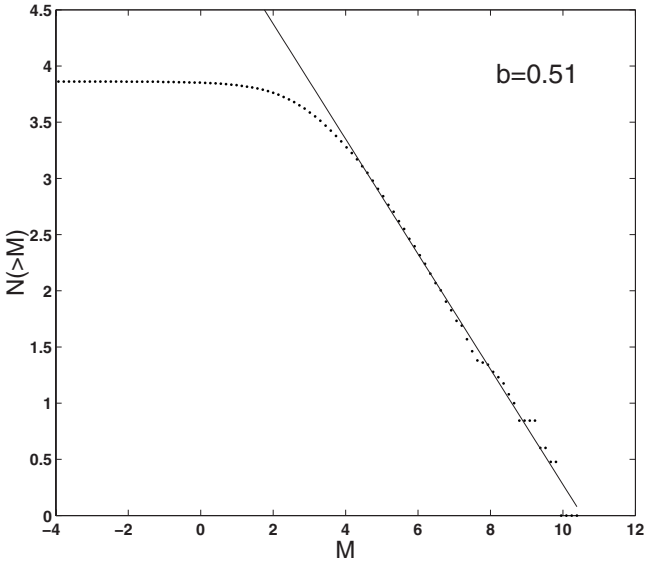

FIG. 9. Number of "electromagnetic earthquakes" (see text) with magnitude M higher than that given by the corresponding abscissa. The continuous line is the least-squares fit of the power law $N(>M)=M^{-b}$, where $b=0.51$. The power law observed here is a fingerprint of an underlying scale-free fracto-electromagnetic activity.

The relevant information is lacking. However, an analysis in terms of traditional empirical GR law leads to a positive answer to the above-mentioned question.

The archetypal power-law found in EQs catalogs is the Gutenberg-Richter magnitude-frequency relationship: the cumulative number of EQs with magnitude greater than M is given by $\log N(>M)=\alpha-bM$. There are increasing reports on premonitory decrease of b value before EQs: foreshock sequences and main shocks are characterized by a much smaller exponent compared to aftershocks, $b\sim 1$ [29]. This behavior represents a statistical average and may not be characteristic of the behavior of individual foreshock sequences.

Figure 9 shows the quantity $N(>A)$ vs EMEQ magnitude M, where $N(>A)$ is the cumulative number of EMEQs with magnitude greater than M. The main part of this distribution is given by $\log N(>M)=\alpha-bM$, where $b\sim 0.5$. We observe that the behavior of the recorded EM earthquakes, associated with activation of a single fault, is in agreement with that of foreshock sequences and main shocks of regional natural seismicity.

GR law also holds for acoustic emission events in rock samples [30]. Acoustic emissions from rock fracturing also show a significant decrease in the level of the observed b values immediately before the critical point. Importantly, laboratory experiments [31] also showed a significant fall of the observed b values from 1 to 0.6 just before the global rupture. Recently, Lei and Satoh [32] presented indicators of critical point behavior prior to rock failure inferred from prefailure damage based on acoustic emission events recorded during the catastrophic fracture of typical rock samples under differential compression. Their results suggest that the prefailure damage evolution is characterized by a dramatic decrease in b value from ~ 1.5 to 0.5 for hard rocks. The above mentioned laboratory findings suggest that the activation of a single fault is a large-scale picture of laboratory seismicity and a small-scale image of natural seismicity.

In laboratory scale, Rabinovitch *et al.* [12] have recently studied the fractal nature of prefracture EM radiation. The cumulative number of EM pulses with amplitude greater than A is given by the law $N(>A)\sim A^{-b}$ with $b=0.62$. Following the analysis in [12] we have shown that the cumulative number of precursory "EM fracto-emissions" with amplitude greater than A is given by $N(>A)\sim A^{-b}$, with a b value of 0.62 [6]. The agreement between the b exponents suggests that the fracturing process is a scale invariant dynamics.

We further focus on this point. The amplitude distribution of the binned data will follow the power-law $N(A)\sim A^{-\zeta}$, where $\zeta=(1+b)$, i.e., $\zeta=1.62$. Remembering that the squared amplitude of the detected EM events is proportional to their energy, the number of EM events with energy between E and $E+dE$ follows the distribution $N(E)\sim E^{-\eta}$, where $\eta=(1+\zeta)/2$, i.e., $\eta=1.31$. The distribution of energies released at any EQ is described by the power law, $N(E)\sim E^{-B}$, where $B\sim 1.4-1.6$. In laboratory scale: (i) Petri *et al.* [33] found a power-law scaling behavior in the acoustic emission energy distribution $N(E)\sim E^{-B}$ with $B=1.3\pm 0.1$; and (ii) Houle and Sethna [34] found that the crumpling of paper generates acoustic pulses with a power-law distribution in energy $P(E)=E^{-B}$, $B=1.3-1.6$; Salminen *et al.* [35] have reported tensile failure experiments on paper sheets. The acoustic emission energy follows power-law distribution with the exponent $B=1.25$. The authors suggest that a large-scale analogy is EQs. The above-mentioned findings suggest that the activation of a single fault is a large-scale picture of laboratory seismicity and a small-scale image of natural seismicity.

VI. ON THE SEISMOGENIC ORIGIN OF THE EM ANOMALY UNDER STUDY

A clear picture of how EQs develop has not emerged yet. On the other hand, it is difficult to prove a correlation between complex events separated in time, such as EQs and their precursors. So, the search for reliable precursors is becoming more and more important in this field of research. Undoubtedly, the problem of EQ prediction is difficult because the source volume inside the Earth is inaccessible to direct observation and because the most important parameter, the stress level, cannot be measured directly. As a result whether an EQ can be predicted or whether an EQ can be preceded by EM precursors are still controversial issues [36]. The present state of research in this field requires a refined definition of a possible preseismic anomaly, and also the development of more objective methods of distinguishing seismogenic EM emissions from nonseismic EM events. We emphasize that we have expressed very clearly our point of view that the occurrence of a sequence of MHz and kHz EM anomalies in the output of the detectors does not qualify by itself as a precursory signal of an important EQ [8]. Our evaluation of the seismogenic origin of a candidate EM precursor is based on a rather austere set of criteria which should be met by a candidate seismogenic EM activity. This

set, which is fully satisfied by the candidate EM precursor associated with the Athens EQ, is constructed as follows.

(1) We first exclude the possibility that the detected signal is a result of man-made noise, geomagnetic activity, or meteorological activity (see Sec. 1E in [8]). If these requirements are satisfied, we proceed to further analysis of the sequence of the detected signals.

(2) Statistical analyses in terms of various organization measures ("block entropy" [14], "Kolmogorov-Sinai entropy" [14], "approximate entropy" [8], and Tsallis entropy) or complexity measures ("correlation dimension" [14] and "T-complexity" [8]) may reveal the launch of the last stages in the EQ preparation process. One cannot find an optimum organization or complexity measure. A combination of some such quantities seems to be the most promising way. All the above-mentioned methods confirm a significant organization increase (or complexity decrease) in the EM bursts A and B. This convergence provides a more reliable detection concerning the launch of a new peculiar phase of the EQ preparation process. However, any statistical analysis even based on a combination of various measures of complexity or organization by itself cannot establish a precursory signal and even more identify a corresponding characteristic stage of the EQ preparation process. Thus further investigation is needed.

(3) EQs are large scale fracture phenomena, so they must obey the physics of the failure process. Two of the pillars of the fracture process, namely the scale invariance and universality, have been projected in the candidate fracto-EM precursor, sharing distinctive statistical properties with natural and laboratory seismicity, such as power-law energy distributions with similar exponents. In Refs. [6,8,14], as well as in this study we have shown that this requirement is really satisfied.

(4) As it is mentioned, a challenge is to distinguish different characteristic epochs in the evolution of candidate precursory EM activity and identify them with equivalent last stages in the fracture-EQ preparation process. In Sec. III we have referred to a relevant two-stage model [5,8]: The MHz EM activity originates during cracking in the heterogeneous component of the focal area. It has been argued that this EM activity could be described in analogy with a thermal continuous phase transition [8]. We stress that a crucial feature of a thermal second-order phase transition is the "symmetry breaking." Importantly, this feature is hidden in the MHz EM emission [8]. The "symmetry breaking" reveals the transition from a sparse almost symmetrical random cracking to a localized cracking zone that includes the backbone of strong asperities. The finally emerged kHz radiation is due to the fracture of the backbone of asperities distributed along the fault sustaining the system [5,8]. This radiation evolves as a phase transition far from equilibrium without any footprint of an equilibrium phase transition [8].

(5) We have paid attention to the peculiar behavior of the EM bursts A and B, which clearly distinguishes them from the whole previously recorded candidate preseismic activity. Indeed, the bursts A and B are characterized not only by a higher organization (or lower complexity) but also by the emergence of persistency [5,8,14]. The appearance of these properties indicates that the process is driven by a positive nonlinear feedback mechanism toward a global instability, acquiring to a great degree the property of irreversibility. Moreover, it is expected that characteristic precursory signals rooted in the fracture process should be projected in the bursts A and B. We have extracted such precursory signatures as follows. Laboratory experiments in terms of acoustic and EM emission verify that the main rupture occurs after the appearance of strong persistent behavior [31,37,38]. Universal indicators of fracture process have been projected to bursts A and B. Natural rock surfaces over a wide range can be represented by fractional Brownian surfaces [39]. The associated Hurst exponent $H \sim 0.7$ to 0.8 has been interpreted as a universal indicator of surface fracture [40]. Maslov *et al.* [41] have formally established that both the temporal and spatial activity can be described as different cuts in the same underlying fractal for a broad range of critical phenomena. We recall that the bursts A and B follow the fractional Brownian motion model, while the associated local H exponents are distributed in the region ~ 0.7 to 0.8 [8]. Notice, the surface of a recently exhumed strike-slip fault plane [42] also follows the fractional Brownian scheme with $H \sim 0.7$ to 0.8. The H exponent specifies the strength of the irregularity ("roughness") of the fBm surface topography: the fractal dimension is calculated from the relation $D=(2-H)$ [43]. Acoustic emission data showed that a larger fractal dimension corresponds to a more stable state of the system, while just prior to failure the fractal dimension decreases quickly to lower values [44]. Lei *et al.* [45] have studied in terms of acoustic emission how an individual asperity fractures, and also the role of asperities in fault nucleation. Their results suggest that the fractal dimension decreases to 1.0–1.4 during asperity fracture. Importantly, in the precursory kHz EM time series under study, the lower D value occurs in the bursts A and B. Characteristically, the second burst B associated with the activation of the main fault is characterized by $D=1.25$. On the other hand, seismological measurements as well as theoretical studies suggest that a surface trace of a single fault might be characterized by $D \sim 1.2$ (Ref. [46] and references therein). Notice that the new field of fractal electrodynamics (Ref. [15] and references therein) indicates that a fracto-EM emission that originates during the formation of a fault having fractal structure should follow a distinct fractal pattern. Such a such distinctive pattern is hidden in the EM precursor under study [15].

(6) The consecutive emerging precursory MHz and kHz EM modes should be in agreement with successive distinct stages of fracture in terms of principles of physical mesomechanics [47]. We have shown that the shift from MHz to kHz EM emission may signal the transition of plastic flow localization from the mesoscale to macroscale culminating in global fracture [17].

(7) A candidate precursory EM activity should be consistent with other precursors that are imposed by data from other disciplines such as seismology, infrared remote sensing [48], synthetic aperture radars interferometry [23], and ultra-low-frequency seismic electric signals (SES), which are ultra-low-frequency (<1 Hz) changes of the electric field of the earth and are consistent with the "pressure stimulated currents model" [49]. This requirement is well-satisfied in the case of the Athens EQ [14]. We emphasize that the syn-

thetic aperture radars interferometry method indicates the activation of two separate faults [23]. This information had also imprinted in the (i) emergence of the two strong kHz EM bursts A and B (see Sec. III and Ref. [22]), (ii) seismic data associated with the Athens EQ [22], and (iii) seismic electric signals (SES) [50]. We further focus on the consistency with the seismic data. Statistical physicists have shown the existence of a power-law-type acceleration of elastic emissions in the laboratory [51] and geophysical scale [52] announcing the global rupture [51]. In Fig. 20 of Ref. [8] we depict the "cumulative Benioff strain release":

$$\epsilon(t) = \sum_i \sqrt{E_i}(t) = A - B(t_f - t)^m \tag{12}$$

computed over a critical circle [52] $R=110$ km at the epicenter of the Athens EQ as a function of time, where t_f is the failure time, E_i is the mechanical energy released by the ith foreshock, and A, B, m are positive quantities (Ref. [8] and references therein). In this figure we also show the "Benioff" cumulative EM energy release $\Sigma A_i(t)$ (in arbitrary units) as a function of time, where A_i is the amplitude of the ith preseismic EM pulse. We draw attention to the similarity of the temporal evolution of both the mechanical and the EM energy release as the main event approaches. This finding suggests a strong correlation between the seismic and EM energy release, i.e., that the detected EM precursor is a subproduct of the Athens fault system generation. Notice that laboratory studies also show: (i) a strong correlation between acoustic and EM pulses during plastic deformation, which is evidence of a common mechanism for both emissions [53], and (ii) that the "Benioff EM energy release" follows a power-law type increase as the global rupture approaches [12]. A recent theoretical study [54] investigates the time-scale invariant changes in EM and mechanical energy releases prior to a large EQ such as that depicted in Fig. 20 of Ref. [8]. The authors suggest that the irreversible thermodynamics with time-scale invariance reveals that the time-scale invariant evolution of damage (such as opening and propagation cracks) produces the observed temporal variation in EM radiation and mechanical energy releases prior to seismic events.

Remark. The candidate precursory sequence of MHz-kHz EM emissions associated with the Athens EQ shows a rather unusual long duration. Furthermore, this signal encompasses a wealth of information related to the Athens's earthquake generation process. A tentative scenario that could explain the special features of our signals is the following. The $M_w = 7.4$ Izmit, Turkey EQ on August 17, 1999 (see Fig. 1 in [55]) triggered widespread regional seismicity in Greece [56]. Characteristically, the onset of a power-law type seismic energy release began immediately after the Izmit EQ (see Fig. 20 in [8]) [56]. One hypothesis is that the surface waves of the Izmit EQ might be responsible for the observed positive feedback [57]. On laboratory scale, Krysac and Maynard [58] have shown that during the fracture of a brittle material, the breaking of a bond launches a propagating stress wave which may trigger the breaking of other bonds. We recall that during the breaking of bonds EM emission is emitted [7,8]. Especially, such a process might be important just prior to an avalanche of bond-breaking events when there would be a relatively high density of bonds on the verge of breaking. Moreover, the surface waves gradually increase the population of cracks. Laboratory experiments [59] demonstrate that preexisting cracks are the most dominant factor of all heterogeneities that govern the faulting process. In this way, the population of preexisting cracks leads to an intense precursory seismicity [8], and thus in a strong precursory EM activity. One might hypothesize that these experimental findings further justify the seismogenic origin of the detected kHz EM emission, as well as the clearly projected in this activity prefracture peculiarities.

(8) In this field of research, first of all, we require that the results can be reproduced. Characteristically, the Chinese experience [60] concerning the behavior of preseismic EM anomalies can be summarized in the following points. (i) The frequency band of the detected EM anomalies is quite wide. (ii) Anomalies are detected earlier in the electric field (MHz) than in the magnetic (kHz) field. (iii) The anomalies stop before the EQ occurs. (iv) No signals are recorded while the EQ is in progress.

(9) A basic reason for our interest in complexity is the striking similarity in behavior close to irreversible phase transition among systems that are otherwise quite different in nature [61]. The appearance in a candidate EM precursor of footprints, which have been evaluated as precatastrophic signs in different well-studied catastrophic events, for example, epileptic seizures or intense magnetic storms, constitutes a supplementary reason to consider the recorded anomaly as a seismogenic emission. Interestingly, theoretical studies suggest that the final and neural-seizure dynamics should have many similar features and could be analyzed within similar mathematical frameworks [62]. We have showed that many similar distinctive precursory symptoms emerge as an important EQ, an epileptic seizure [16,63], or an intense magnetic storm [64] is approaching. More precisely, we show that a combination of a significant increase in organization, a remarkable acceleration of energy release manifested in the increase in susceptibility, and a transition from antipersistent (negative feedback) to persistent (positive feedback) behavior indicates that the occurrence of an epileptic seizure/intense magnetic storm/EQ is imminent. In our opinion, it is very difficult for a nonseismogenic-electromagnetic emission to obey such a multidisciplinary scheme.

Finally, we comment on two peculiarities associated with the recorded candidate precursory EM emissions. Aftershocks universally occur after crustal EQs. Our data reveal a lack of EM anomalies during the aftershocks. We focus on this point. In order to have the possibility to evaluate a recorded EM anomaly as a precursory signal it should be "emerging" clearly from the EM background. This means that the detected EM radiation should have not been significantly absorbed by conducting layers of the crust or by the much more conductive sea [8]. Moreover, it should have a long duration, that is, from a few hours up to a few days, in order to use the measurements for statistical purposes. These requirements imply that a useful EM precursor should be linked to an on-land seismic event which is both strong, i.e., with magnitude ~6 or greater, and shallow [8]. In this case

we have reasons to assert that the fracture process is extended up to the surface layer of the crust, and thus the captured precursory EM emissions are produced by a population of EM emitters (opening cracks) that is sufficient to represent the behavior of the total number of the activated cracks during the evolution of fracture [8]. Aftershocks satisfy several empirical laws, among them, the Bath's law, which states that the differences Δm in magnitudes between mainshocks and their largest aftershocks are approximately constant, i.e., $\Delta m \sim 1.2$, regardless of the magnitudes of the mainshocks [65]. In harmony with the Bath's law, the largest aftershock associated with the Athens EQ was 4.9. This observation probably supports the lack of EM anomalies in our data during the aftershocks. On the other hand, if someone follows the daily background pattern of the kHz recordings one finds the existence of a minimum around mid-day (see Fig. 2). We clarify that the observed slow daily variation refers to the EM background, i.e., to the natural EM emission. This natural emission depends mostly on sources rooted in atmosphere and ionosphere (see p. 46 in [66]) propagating through the waveguide formed by the conductive Earth's surface and ionosphere. The origination of this daily variation is thought to be the fact that the night-time radiation, due to transverse EM propagation mode (TEM), is more intense than the daytime radiation and changes daily because the absorption in the ionosphere decreases with the decreased density of ions and electrons at night (see p. 162 in [62]). We point out that the rapidly changing candidate precursory emission, sampled at 1 Hz, is added to the above-mentioned slowly changing EM background.

VII. CONCLUSIONS

Experimental evidence indicates that the nonextensive q-Tsallis statistics describes not only regional seismicities, each of them covering many geological faults, but also the "electromagnetic seismicity" associated with the activation of a single geological fault. Importantly, similar q values, which measure the nonextensivity, describe the energy distribution of EQs in a seismic region, as well as the distribution of the "electromagnetic earthquakes" associated with the activation of a single EQ. A pillar of fracture is the universality of its fractal properties [27,39,40,67]. Thus the aforementioned finding could be considered as a further indication of the universality of fractal properties among a large number of geological processes [27,39,40,67]: it suggests that the statistics of seismicity in a seismic region is merely a macroscopic reflection of the physical processes in a particular EQ source. Importantly, in Ref. [12] we have shown that the statistics of laboratory seismicity in terms of EM emission is a microscopic reflection of the physical processes in a particular EQ source. This evidence further supports the hypothesis that the explanation of Eqs. (6) and (7) by the precursory EM data is possibly rooted in the above-mentioned universality of fractal properties of the fracture. Moreover, the obtained formulas in Refs. [1,2] are not a mere fitting artifact, and that a more exhaustive study of the nonextensive Tsallis statistics and its relation with the fracture process is needed. Finally, the evolution of the q-Tsallis entropy into PEM time series quantifies and visualizes temporal changes of the organization as the EQ approaches. Importantly, it discriminates a distinctive epoch in the tail of the PEM activities, which is characterized by a significant increase of the organization. Recent studies indicate that the transition to this epoch is accompanied by the appearance of strong persistency, as well as by the absence of any footprint of an equilibrium phase transition. It might be concluded that this epoch reflects the faulting nucleation phase of the EQ preparation, namely, the fracture of fragments that fill the gap between the two rough profiles of the corresponding activated fault. The excellent description of the "EM earthquakes" associated with the activation of a single fault by the nonextensive formulas [Eqs. (6) and (7)] strongly supports this hypothesis.

ACKNOWLEDGMENT

The project was co-funded by the European Social Fund and National Resources—(EPEAEK II) PYTHAGORAS (70/3/7357).

[1] O. Sotolongo-Costa and A. Posadas, Phys. Rev. Lett. **92**, 048501 (2004).
[2] R. Silva, G. S. Franca, C. S. Vilar, and J. S. Alcaniz, Phys. Rev. E **73**, 026102 (2006).
[3] V. DeRubeis, R. Hallgass, V. Loreto, G. Paladin, L. Pietronero, and P. Tosi, Phys. Rev. Lett. **76**, 2599 (1996).
[4] Mechanical and Electromagnetic Phenomena Accompanying Preseismic Deformation, From Laboratory to Geophysical Scale, edited by K. Eftaxias, V. Sgrigna, and T. Chelidze, special issue of Tectonophysics **431**(1–4) (2007).
[5] P. G. Kapiris, K. A. Eftaxias, and T. L. Chelidze, Phys. Rev. Lett. **92**, 065702 (2004).
[6] P. Kapiris, G. Balasis, J. Kopanas, G. Antonopoulos, A. Peratzakis, and K. Eftaxias, Nonlinear Processes Geophys. **11**, 137 (2004).
[7] Y. F. Contoyiannis, P. G. Kapiris, and K. A. Eftaxias, Phys. Rev. E **71**, 066123 (2005).
[8] K. Karamanos, D. Dakopoulos, K. Aloupis, A. Peratzakis, L. Athanasopoulou, S. Nikolopoulos, P. Kapiris, and K. Eftaxias, Phys. Rev. E **74**, 016104 (2006).
[9] E. Sharon, S. P. Gross, and J. Fineberg, Phys. Rev. Lett. **74**, 5096 (1995); E. Sharon and J. Fineberg, Nature (London) **397**, 333 (1999); Phys. Rev. B **54**, 7128 (1996).
[10] S. C. Langford, D. L. Doering, and J. T. Dickinson, Phys. Rev. Lett. **59**, 2795 (1987); J. Dickinson, S. Langford, L. Jensen, G. McVay, J. Kelso, and C. Pantano, J. Vac. Sci. Technol. A **6**, 1084 (1988); T. Miura and K. Nakayama, J. Appl. Phys. **88**, 5444 (2000); A. Gonzalez and C. Pantano, Appl. Phys. Lett. **57**, 246 (1990).
[11] D. Bahat, A. Rabinovitch, and V. Frid, *Tensile Fracturing in*

Rocks. Tectonofractographic and Electromagnetic Radiations Method (Springer, Heidelberg, 2005); U. Nitsan, Geophys. Res. Lett. **4**, 333 (1977); T. Ogawa, K. Oike, and T. Miura, J. Geophys. Res., [Solid Earth Planets] **90**, 6245 (1985); J. Muto, H. Nagahama, T. Miura, and I. Arakawa, Tectonophysics **431**, 113 (2007).

[12] A. Rabinovitch, V. Frid, and D. Bahat, Phys. Rev. E **65**, 011401 (2001).

[13] M. Gokhberg, V. Morgounov, and O. Pokhotelov, *Earthquake Prediction, Seismo-Electromagnetic Phenomena* (Gordon and Breach, Singapore, 1995).

[14] K. Karamanos, A. Peratzakis, P. Kapiris, S. Nikolopoulos, J. Kopanas, and K. Eftaxias, Nonlinear Processes Geophys. **12**, 835 (2005).

[15] K. Eftaxias, P. Frangos, P. Kapiris, J. Polygiannakis, J. Kopanas, and A. Peratzakis, Fractals **12**, 243 (2004).

[16] P. Kapiris, J. Polygiannakis, X. Li, X. Yao, and K. Eftaxias, Europhys. Lett. **69**, 657 (2005).

[17] K. Eftaxias, V. E. Panin, and Ye. Deryugin, Tectonophysics **431**, 273 (2007).

[18] C. Tsallis, J. Stat. Phys. **52**, 479 (1988); E. M. F. Curado and C. Tsallis, J. Phys. A **24**, L69 (1991); **24**, L69 (1991); **25**, 1019 (1992); in *Nonextensive Statistical Mechanics and its Applications*, edited by S. Abe and Y. Okamoto (Springer Verlag, Berlin, 2001).

[19] V. G. Kossobokov, V. I. Keilis-Borok, and B. Cheng, Phys. Rev. E **61**, 3529 (2000); D. Sornette and A. Helmstetter, Phys. Rev. Lett. **89**, 158501 (2002).

[20] S. Abe and G. B. Bagci, Phys. Rev. E **71**, 016139 (2005).

[21] C. S. Vilar, G. S. Franca, R. Silva, and J. S. Alcaniz, Physica A **377**, 285 (2007).

[22] K. Eftaxias, P. Kapiris, J. Polygiannakis, N. Bogris, J. Kopanas, G. Antonopoulos, A. Peratzakis, and V. Hadjicontis, Geophys. Res. Lett. **28**, 3321 (2001).

[23] C. Kontoes, P. Elias, O. Sycioti, P. Briole, D. Remy, M. Sachpazi, G. Veis, and I. Kotsis, Geophys. Res. Lett. **27**, 3989 (2000).

[24] J. P. Sethna, K. A. Dahmen, and C. R. Myers, Nature (London) **410**, 242 (2001), and references therein.

[25] C. Tsallis, Phys. Rev. E **54**, R2197 (1996); **58**, 1442 (1998).

[26] I. V. Karlin, M. Grmela, and A. N. Gorban, Phys. Rev. E **65**, 036128 (2002); R. Silva and J. S. Alcaniz, Phys. Lett. A **313**, 393 (2003); P. Leubner, Astrophys. J. **604**, 469 (2004); G. Kaniadakis, M. Lissia, and A. M. Scarfone, Phys. Rev. E **71**, 046128 (2005); R. Silva and J. A. S. Lima, *ibid.* **72**, 057101 (2005); X. Yang, S. Du, and J. Ma, Phys. Rev. Lett. **92**, 228501 (2004).

[27] P. Bak, C. Tang, and K. Wiesenfeld, Phys. Rev. Lett. **59**, 381 (1987); P. Bak and C. Tang, J. Geophys. Res. **94**, 15635 (1989); P. Bak, *How Nature Works: The Science of Self-Organized Criticality* (Copernicus, New York, 1996); D. Sornette, *Critical Phenomena in Natural Sciences: Chaos, Fractals, Selforganization, and Disorder: Concepts and Tools* (Springer, Heidelberg, 2004).

[28] B.-L. Hao, *Elementary Symbolic Dynamics and Chaos in Dissipative Systems* (Word Scientific, Singapore, 1989); Physica D **51**, 161 (1991); W. Ebeling and G. Nicolis, Chaos, Solitons Fractals **2**, 635 (1992); D. Lind and B. Marcus, *An Introduction to Symbolic Dynamics and Coding* (Cambridge University Press, Cambridge, England, 1995).

[29] S. Hainzl, G. Zoller, and F. Scherbaum, Geophys. Res. Lett. **108**, 2013 (2003); L. Knopoff, Proc. Natl. Acad. Sci. U.S.A. **97**, 11880 (2000).

[30] C. Scholz, Bull. Seismol. Soc. Am. **58**, 399 (1968).

[31] A. Ponomarev, A. Zavyalov, V. Smipnov, and D. Lockner, Tectonophysics **277**, 57 (1997).

[32] X. Lei and T. Satoh, Tectonophysics **431**, 97 (2007).

[33] A. Petri, G. Paparo, A. Vespignani, A. Alippi, and M. Costantini, Phys. Rev. Lett. **73**, 3423 (1994).

[34] P. A. Houle and J. P. Sethna, Phys. Rev. E **54**, 278 (1996).

[35] L. I. Salminen, A. I. Tolvanen, and M. J. Alava, Phys. Rev. Lett. **89**, 185503 (2002).

[36] R. J. Geller, Geophys. Res. Lett. **23**, 1291 (1996); R. J. Geller, D. D. Jackson, Y. Y. Kagan, and F. Mulargia, Science **275**, 1616 (1997).

[37] X. Lei, K. Masuda, O. Nishizawa, L. Jouniaux, L. Liu, W. Ma, T. Satoh, and K. Kusunose, J. Struct. Geol. **26**, 247 (2004).

[38] X. Lei, O. Nishizawa, K. Kusunose, A. Cho, and T. Satoh, Tectonophysics **328**, 329 (2000).

[39] J. Huang and D. Turcotte, Earth Planet. Sci. Lett. **91**, 223 (1988); D. Turcotte, *Fractals and Chaos in Geology and Geophysics*, 2nd ed. (Cambridge University Press, Cambridge, England, 1997).

[40] J. M. Lopez and J. Schmittbuhl, Phys. Rev. E **57**, 6405 (1998); A. Parisi and R. C. Ball, Phys. Rev. B **72**, 054101 (2005); L. Ponson, D. Bonamy, and E. Bouchaud, Phys. Rev. Lett. **96**, 035506 (2006).

[41] S. Maslov, M. Paczuski, and P. Bak, Phys. Rev. Lett. **73**, 2162 (1994).

[42] F. Renard, C. Voisin, D. Marsan, and J. Schmittbuhl, Geophys. Res. Lett. **33**, L04305 (2006).

[43] C. Heneghan and G. McDarby, Phys. Rev. E **62**, 6103 (2000).

[44] X.-T. Feng and M. Seto, Geophys. J. Int. **136**, 275 (1999); P. R. Sammonds, P. G. Meredith, and I. G. Main, Nature (London) **359**, 228 (1992).

[45] X. Lei and T. Satoh, Tectonophysics **431**, 97 (2007).

[46] M. Sahimi, M. C. Robertson, and C. G. Sammis, Phys. Rev. Lett. **70**, 2186 (1993).

[47] V. E. Panin, Theor. Appl. Fract. Mech. **30**, 1 (1998); **37**, 261 (2001).

[48] D. Ouzounov and F. T. Freund, Adv. Space Res. **33**, 268 (2004); S. A. Pulinetes and K. Boyarchuk, *Ionospheric Precursors of Earthquakes* (Springer, Heidelberg, 2004); C. Filizzola, N. Pergola, C. Pietrapertosa, and V. Tramutoli, Phys. Chem. Earth, Part B **29**, 517 (2004).

[49] P. Varotsos, *The Physics of Seismic Electric Signals* (TerraPub, Tokyo, 2005).

[50] P. Varotsos, K. Eftaxias, V. Hadjicontis, N. Bogris, E. Skordas, P. Kapiris, and M. Lazaridou, Acta Geophys. Pol. **47**, 435 (1999).

[51] D. Sornette and C. Sammis, J. Phys. I **5**, 607 (1995); A. Johansen and D. Sornette, Eur. Phys. J. B **18**, 163 (2000).

[52] D. Bowman, G. Quillon, C. Sammis, A. Sornette, and D. Sornette, J. Geophys. Res. **103**, 24359 (1998); C. G. Sammis and D. Sornette, Proc. Natl. Acad. Sci. U.S.A. **99**, 2501 (2002).

[53] C. Mavromatou, V. Hadjicontis, D. Ninos, D. Mastroyiannis, E. Hadjicontis, and K. Eftaxias, Phys. Chem. Earth, Part B **29**, 353 (2004).

[54] Y. Kawada, H. Nagahama, and N. Nakamura, Nat. Hazards Earth Syst. Sci. **7**, 599 (2007).

[55] P. Kapiris, K. Nomicos, G. Antonopoulos, J. Polygiannakis, K. Karamanos, J. Kopanas, A. Zissos, A. Peratzakis, and K. Eftaxias, Earth, Planets Space **57**, 215 (2005).
[56] E. Brodsky, V. Karakostas, and H. Kanamori, Geophys. Res. Lett. **27**, 2741 (2000); A. Tzanis and K. Makropoulos, Natural. Hazards **27**, 85 (2002); G. Papadopoulos, Bull. Seismol. Soc. Am. **92**, 312 (2002).
[57] R. Stein, Nature (London) **402**, 605 (1999).
[58] L. C. Krysac and J. D. Maynard, Phys. Rev. Lett. **81**, 4428 (1998).
[59] H. Li, Z. Jia, Y. Bai, M. Xia, and F. Ke, Pure Appl. Geophys. **159**, 1933 (2002).
[60] S. Qian, J. Yian, H. Cao, S. Shi, Z. Lu, J. Li, and K. Ren, in *Electromagnetic Phenomena Related to Earthquake Prediction*, edited by M. Hayakawa and Y. Fujinawa (Terrapub, Tokyo, 1994), pp. 205–211.
[61] H. E. Stanley, Rev. Mod. Phys. **71**, S358 (1999); T. Vicsek, Nature (London) **418**, 131 (2002).
[62] J. Hopfield, Phys. Today **47**(2), 40 (1994); A. V. M. Herz and J. J. Hopfield, Phys. Rev. Lett. **75**, 1222 (1995); J. B. Rundle, W. Klein, S. Gross, and D. L. Turcotte, *ibid.* **75**, 1658 (1995).
[63] K. Eftaxias, P. Kapiris, G. Balasis, A. Peratzakis, K. Karamanos, J. Kopanas, G. Antonopoulos, and K. Nomicos, Nat. Hazards Earth Syst. Sci. **6**, 205 (2006).
[64] G. Balasis, I. A. Daglis, P. Kapiris, M. Mandea, D. Vassiliadis, and K. Eftaxias, Ann. Geophys. **24**, 3557 (2006).
[65] R. Shcherbakov and D. Turcotte, Bull. Seismol. Soc. Am. **94**, 1968 (2004).
[66] M. Hata and S. Yabashi, in *Electromagnetic Phenomena Related to Earthquake Prediction*, edited by M. Hayakawa and Y. Fujinawa (TerraPub, Tokyo, 1994), pp. 159–174.
[67] J. Huang and D. Turcotte, Earth Planet. Sci. Lett. **91**, 223 (1988); E. Bonnet, O. Bour, N. E. Odling, P. Davy, I. Main, P. Cowie, and B. Berkowitz, Rev. Geophys. **39**, 347 (2001); J. B. Rundle, D. Turcotte, R. Shcherbakov, W. Klein, and C. Sammis, *ibid.* **41**, 1019 (2003).